


RESEARCH ARTICLE

10.1002/2017MS001099

Ocean Modeling on a Mesh With Resolution Following the Local Rossby Radius

Dmitry V. Sein^{1,2} , Nikolay V. Koldunov^{1,3}, Sergey Danilov^{1,4,5}, Qiang Wang¹ , Dmitry Sidorenko¹, Irina Fast⁶, Thomas Rackow¹ , William Cabos⁷, and Thomas Jung^{1,8}

Key Points:

- Ocean model resolution following the local Rossby radius: advantages and disadvantages
- Resolving the Rossby radius alone in ocean models is insufficient and the use of a priori information on eddy dynamics is required

Correspondence to:

D. Sein,
dmitry.sein@awi.de

Citation:

Sein, D. V., Koldunov, N. V., Danilov, S., Wang, Q., Sidorenko, D., Fast, I., . . . Jung, T. (2017). Ocean modeling on a mesh with resolution following the local Rossby radius. *Journal of Advances in Modeling Earth Systems*, 9. <https://doi.org/10.1002/2017MS001099>

Received 21 JUN 2017

Accepted 19 OCT 2017

Accepted article online 27 OCT 2017

¹Alfred Wegener Institute, Helmholtz Centre for Polar and Marine Research, Bremerhaven, Germany, ²P. P. Shirshov Institute of Oceanology RAS, St. Petersburg, Russia, ³MARUM—Center for Marine Environmental Sciences, Bremen, Germany, ⁴A. M. Obukhov Institute of Atmospheric Physics RAS, Moscow, Russia, ⁵Department of Mathematics and Logistics, Jacobs University, Bremen, Germany, ⁶DKRZ, German Climate Computing Centre, Hamburg, Germany, ⁷Department of Physics and Mathematics, University of Alcala, Alcala, Spain, ⁸Institute of Environmental Physics, University of Bremen, Bremen, Germany

Abstract We discuss the performance of the Finite Element Ocean Model (FESOM) on locally eddy-resolving global unstructured meshes. In particular, the utility of the mesh design approach whereby mesh horizontal resolution is varied as half the Rossby radius in most of the model domain is explored. Model simulations on such a mesh (FESOM-XR) are compared with FESOM simulations on a smaller-size mesh, where refinement depends only on the pattern of observed variability (FESOM-HR). We also compare FESOM results to a simulation of the ocean model of the Max Planck Institute for Meteorology (MPIOM) on a tripolar regular grid with refinement toward the poles, which uses a number of degrees of freedom similar to FESOM-XR. The mesh design strategy, which relies on the Rossby radius and/or the observed variability pattern, tends to coarsen the resolution in tropical and partly subtropical latitudes compared to the regular MPIOM grid. Excessive variations of mesh resolution are found to affect the performance in other nearby areas, presumably through dissipation that increases if resolution is coarsened. The largest improvement shown by FESOM-XR is a reduction of the surface temperature bias in the so-called North-West corner of the North Atlantic Ocean where horizontal resolution was increased dramatically. However, other biases in FESOM-XR remain largely unchanged compared to FESOM-HR. We conclude that resolving the Rossby radius alone (with two points per Rossby radius) is insufficient, and that careful use of a priori information on eddy dynamics is required to exploit the full potential of ocean models on unstructured meshes.

1. Introduction

Eddy-permitting and eddy-resolving ocean simulations are becoming more and more common in climate studies. Eddies modulate numerous processes in the ocean, such as lateral spreading of heat or salt and interaction of the flow with topography. There are indications that increased ocean resolution may contribute to the reduction of sea surface temperature biases and to improvements in the representation of ocean heat transport (see, e.g., Griffies et al., 2015; Hewitt et al., 2016; Roberts et al., 2016; Small et al., 2014). In order to maintain mesoscale eddy dynamics in a model, it is widely assumed that ocean grids need to resolve the first internal Rossby radius of deformation locally. In fact, Hallberg (2013) demonstrates that a resolution of two grid intervals per Rossby radius marks a sharp boundary between noneddying and eddy-permitting regimes, implying that a resolution finer than that should be aimed for by eddy-resolving models.

The Rossby radius of deformation in the ocean generally decreases with increasing latitude. The resolution of ocean circulation models using quasi-Mercator grids partly follows this tendency. However, even grids with nominal resolution of $1/12^\circ$ at the equator remain only eddy-permitting in certain regions at high latitudes (e.g., most of the Arctic Ocean). A new generation of models formulated on unstructured meshes offer more flexibility in designing meshes. For example, it is possible to vary the horizontal resolution locally so that the grid cell size follows the local Rossby radius. Such models have matured sufficiently (e.g., Danilov et al., 2004; Ringler et al., 2013; Wang et al., 2014) and already serve as valuable tools in climate research (e.g., Rackow et al., 2016; Sidorenko et al., 2015).

© 2017. The Authors.

This is an open access article under the terms of the Creative Commons Attribution-NonCommercial-NoDerivs License, which permits use and distribution in any medium, provided the original work is properly cited, the use is non-commercial and no modifications or adaptations are made.

However, the question of what is the best strategy for selecting horizontal model resolution remains open. The flexibility of unstructured meshes gives a wide range of possible options for mesh design including, for example, the classical quasi-Mercator approach with grid refinement toward the poles, construction of complicated functions according to ocean bathymetry or SSH variability (Sein et al., 2016) or adjusting resolution following the local Rossby radius (for an illustration refer to Figure 1 from Hallberg, 2013). Moreover, there is the option to combine several approaches. There are two potential issues when it comes to designing unstructured meshes. First, as shown by Danilov and Wang (2015), the proximity of coarse and fine areas on a single mesh may have consequences for the high-resolution part. This is because eddies can be damped in high-resolution regions if their dynamics depends on upstream perturbations coming from nearby regions that employ coarse resolution. Second, dissipative parameters such as viscosity and lateral

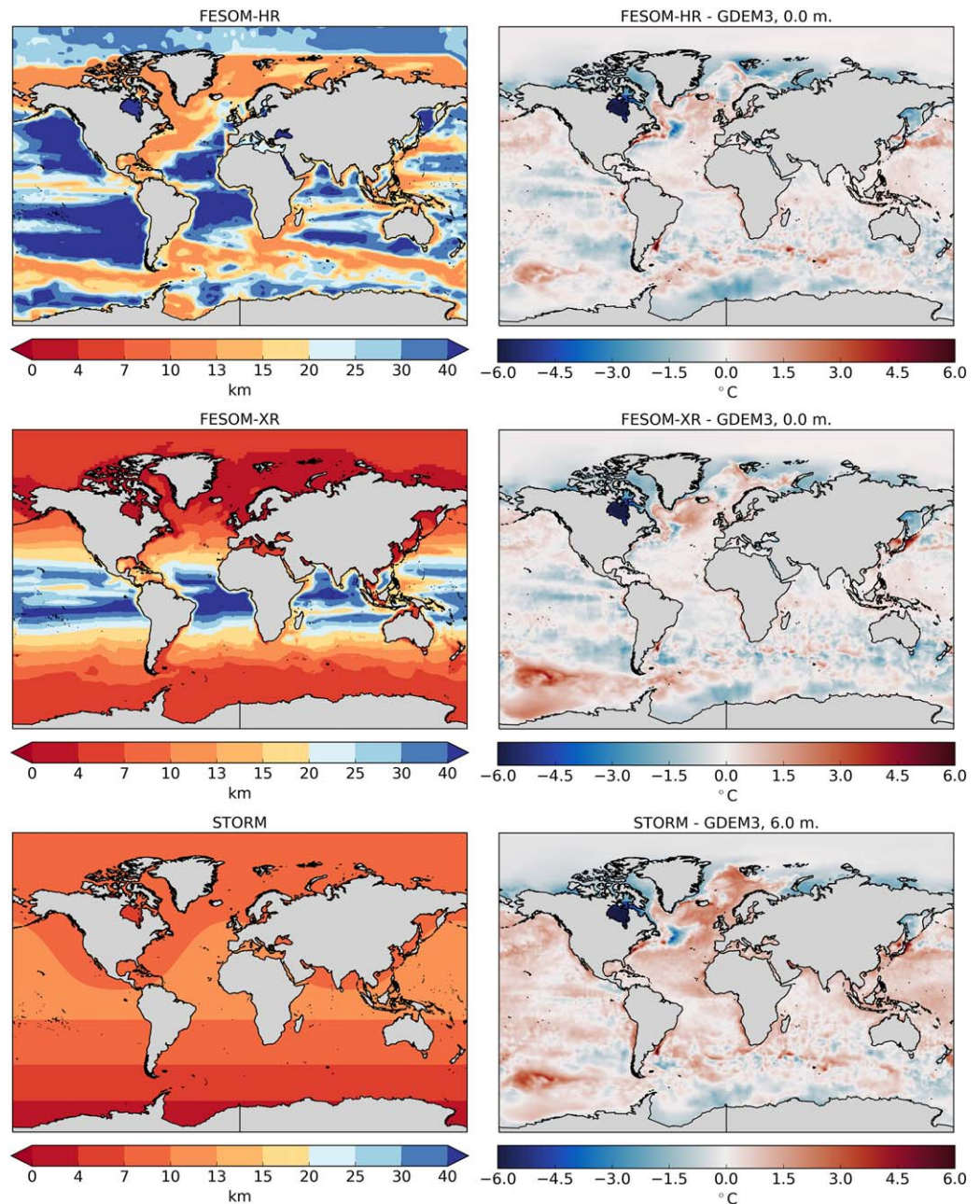


Figure 1. (left in km) Spatial distribution of horizontal resolution of the ocean model grids used in this study (right) along with model sea surface temperature (SST in °C) biases relative to GDEM3 climatology (Carnes, 2009).

diffusivity are scaled on variable resolution meshes according to the mesh cell size—a coarser mesh, even if it locally resolves the Rossby radius, may thus imply enhanced local dissipation which will suppress eddy dynamics.

This manuscript is a follow-up study to Sein et al. (2016), which suggested to use the observed SSH variance pattern to define regions of refined resolution of unstructured meshes. In the current work, we employ a resolution dependence that is based on the Rossby radius and that results in a multiresolution ocean grid (XR) with a number of degrees of freedom (the number of mesh vertices) comparable to a more conventional 1/10° global grid. On the XR mesh, the resolution over a substantial part of the ocean area follows the main criterion of two grid intervals per local Rossby radius; it is further refined in some areas based on the patterns of observed variability but is capped at 4 km in the Northern Hemisphere and at 7 km in the Southern Hemisphere, resulting in a mesh size that is still manageable for currently available high performance computing systems. We discuss the resolution/dissipation dichotomy and show that locally resolving the Rossby radius alone is not necessarily sufficient for maintaining eddy dynamics at a level similar to that known from observations, because the dependence of dissipation on resolution affects eddy dynamics on its own.

In summary, the purpose of this study is to address the following questions:

1. What do we gain by using a mesh design strategy based not only on ocean variability, but also on the local Rossby radius?
2. How does such a “quasi eddy-resolving mesh” compare to ocean simulations by a structured-mesh model with a similar amount of degrees of freedom (but nearly uniformly distributed in space)?

To answer these questions, we compare FESOM-XR simulation to FESOM simulations on a smaller mesh that is refined according to the pattern of observed sea surface height variability (FESOM-HR, Sein et al. 2016) and to a simulation on a regular mesh carried out with the Max Planck Institute Ocean Model (MPIOM).

The structure of the paper is as follows: in section 2, we describe the configuration of the setups used; section 3 presents the discussion, with focus on the simulated variability in areas with strong eddy activity; the last section gives a discussion and provides conclusions.

2. Simulations and Methods

2.1. FESOM at Medium and High Resolution

Model simulations used in this study are summarized in Table 1. Two of them were carried out using the Finite Element Sea Ice-Ocean Model (FESOM1.4, Wang et al., 2014) and have different multiresolution meshes. The first mesh, with medium high resolution (FESOM-HR) has approximately 1.3×10^6 wet surface nodes (vertices) and roughly matches the size of a 1/4° quasi-Mercator mesh ($\sim 1.5 \times 10^6$ surface nodes, of which about 10^6 are wet points). The second, “eXtremely” high-resolution mesh (FESOM-XR) has about 5×10^6 wet surface nodes and is close in size to a 1/10° quasi-Mercator mesh (about 5.6×10^6 wet points). The mesh resolution, defined as the square root of twice the area of the triangles is shown in Figure 1 (left). The resolution of both FESOM meshes varies considerably, ranging from 10 to 60 km in HR and from 4 to 60 km in XR. The principles underlying the mesh design will be explained in detail in section 2.3. Both FESOM simulations are driven by the CORE-II forcing (Large & Yeager, 2009) and run over a period of 1948–2007.

Table 1
Basic Parameters of Models Used in the Study

Simulation	Model	Number of wet surface points (degrees of freedom)	Atmospheric forcing	Period
FESOM-HR	FESOM 1.4	1.3×10^6	CORE II	1948–2007
FESOM-XR	FESOM 1.4	5.0×10^6	CORE II	1948–2007
STORM	MPIOM	5.6×10^6	NCEP/NCAR reanalysis-1	1948–2010

The Gent-McWilliams (GM) parameterization (Gent & McWilliams, 1990) for eddy stirring in FESOM is used in a default mode for FESOM-HR simulation. In this mode, it is smoothly switched off within the resolution range from 50 to 25 km. In the FESOM-XR run, the GM parameterization was switched off for the whole ocean. Both meshes use 47 unevenly spaced z-levels in the vertical, with spacing increasing from 10 m at the surface to ~500 m in the deepest layers.

Figure 2 shows 5 day mean snapshots of velocity (in logarithmic scale) at 100 m depth in the FESOM-XR simulation. All major current systems of the global ocean are reproduced and strong eddy activity along the main separation zones of western boundary currents and the Antarctic Circumpolar Current (ACC) front is clearly visible. The major current systems in the Arctic Ocean are also well represented.

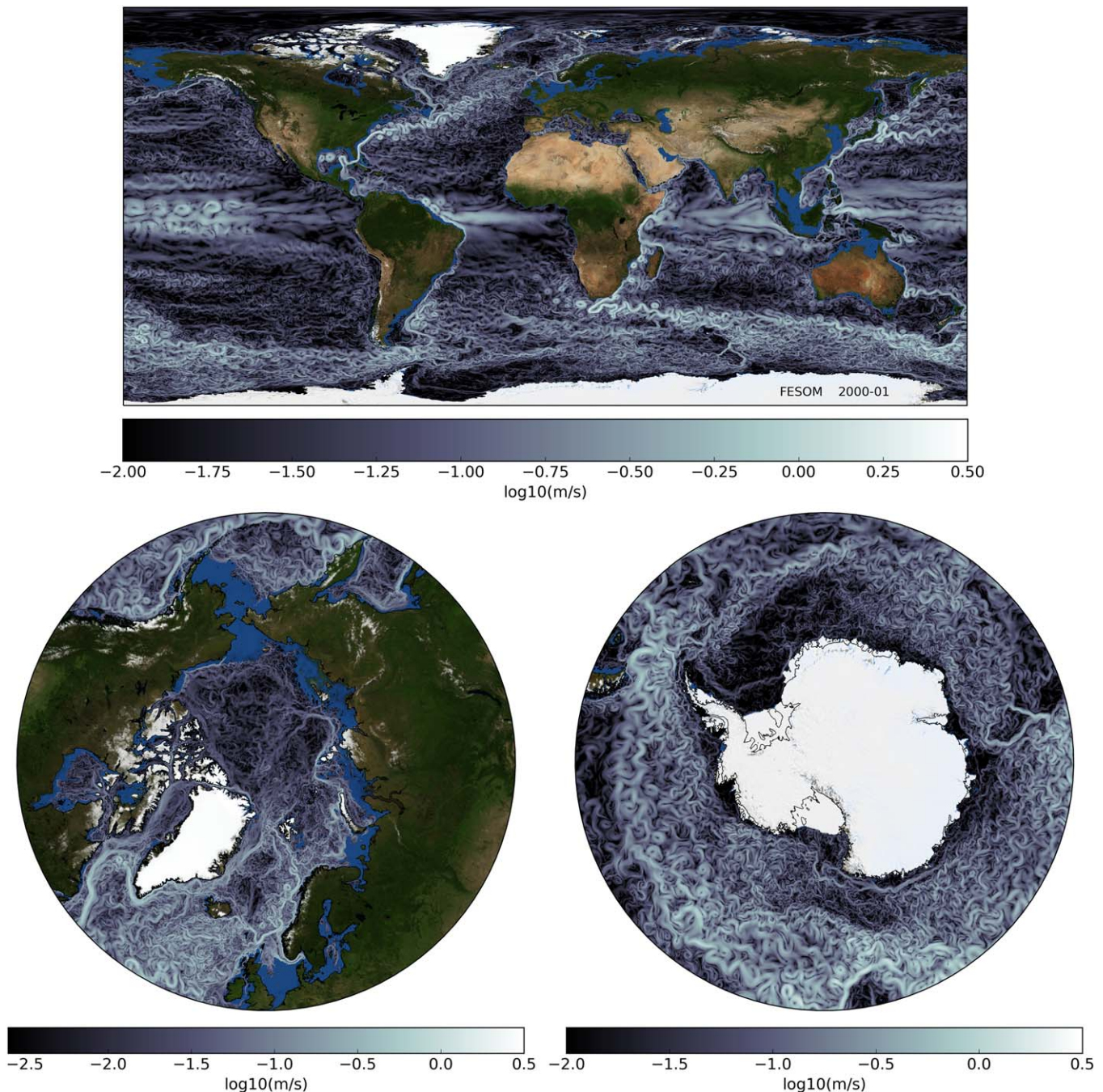


Figure 2. Five daily mean snapshots of velocity (in logarithmic scale) at 100 m depth in the FESOM-XR simulation.

2.2. Storm

The STORM simulation is a global high-resolution configuration of the Max Planck Institute Ocean Model (MPIOM, Marsland et al., 2002). It uses a tripolar grid with a nominal resolution of $1/10^\circ$ around the equator that increases toward the grid poles located in North America, Eurasia, and over Antarctica. The actual grid resolution is shown in Figure 1 (bottom). It is the highest in the Southern Ocean, where it reaches 3–4 km in narrow coastal regions in the Weddell and the Ross Seas. There are 80 z-levels in the vertical, with spacing increasing from 10 to 15 m in the upper 200 m to about 300 m in the deeper layers. The model was forced by the NCEP/NCAR reanalysis-1 (Kalnay et al., 1996) data for the period 1948–2010. Similar to the FESOM-XR simulation, the parameterization of eddy stirring is switched off for the whole ocean. Further information on the STORM simulation can be found in von Storch et al. (2012) and Li and von Storch (2013).

2.3. Mesh Design Principles

The design of the FESOM-HR mesh was presented and validated in Sein et al. (2016). It is based on the idea of using finer resolution, and hence computational resources, in those regions where observed eddy variability is high. For this purpose, we use the pattern of sea surface height (SSH) variance derived from satellite altimetry (AVISO). This pattern is filtered to preserve the large-scale components and used as a basis for the mesh design. The resolution in FESOM-HR is set to be ~ 10 km in places of high variability, including the western boundary currents and ACC; and it is smoothly coarsened to the background resolution of 60 km in areas with relatively weak variability (see Sein et al., 2016, for details). The mesh is additionally refined in the vicinity of coastlines and in certain passages (e.g., 2 km in the Strait of Gibraltar).

If one requires that the total number of nodes is less than the computationally affordable maximum N , the transitions between the eddy-resolving patches and coarse areas turn out to be relatively sharp, if N amounts to less than $\sim 2 \times 10^6$. This limit of N roughly matches the number of nodes for a regular $1/4^\circ$ ocean mesh, which can be considered as the current goal for global climate modeling. The close proximity of coarser mesh regions may effectively damp eddies each time they encounter the coarser mesh elements, which would result in a reduction of the efficient resolution. An additional caveat is in the implementation of the GM parameterization which is resolution-dependent. Being active in the areas of coarse and intermediate resolution it may damp the eddy dynamics in the refined regions, which significantly relies on perturbations coming from the outside.

The main criticism of the approach above is that a single target resolution (10 km in this particular case) for the areas of high observed eddy variability can perhaps be a good option for the most intense western boundary currents, but it has to be adjusted for weaker eddies encountered in other regions such as in high latitudes. More generally, one expects that the eddy dynamics and hence the resolution has to be related to the Rossby radius of deformation. According to Hallberg (2013), the transition between eddy-permitting and eddy-resolving meshes is marked by the resolution of two grid intervals per the first internal Rossby radius. Note that this is only a lower boundary, and even finer resolution might be needed to fully model mesoscale eddy dynamics (see, e.g., Soufflet et al. 2016, where eddy kinetic energy spectra are compared as function of resolution). In order to obtain manageable mesh sizes, we take it as a basic principle in this study, although we hypothesize already that it may need further adjustments, especially on highly variable meshes.

In summary, the FESOM-XR mesh is based on varying resolution equal to half of the local Rossby radius, which is capped at 4 km (7 km) in the Northern Hemisphere (Southern Hemisphere). The Rossby radius is calculated using the PHC3 climatology (Steele et al., 2001). Since the equatorial Rossby radius is rather large, an upper bound of 60 km is employed for the coarsest resolution. This basic resolution is further improved in some key regions by refinement relying on the observed high SSH variability. In other words, the resolution of the FESOM-XR mesh is designed using a combination of two criteria. The first one is to enforce a grid size of half the Rossby radius, and the second one (mainly equatorial and tropical regions) is to scale the grid size by observed SSH variability. There are other necessary resolution adjustments on the FESOM-XR mesh, but they are of geometrical character aiming at resolving the geometry of some passages. Although they introduce grid cell sizes smaller than 4 km (e.g., 2 km in the Strait of Gibraltar), they are of less relevance to this study and will not be discussed further. Because of relatively high-resolution upper bounds for refinement used in high latitudes (4 and 7 km), the total number of nodes on the FESOM-XR mesh turns out to be much larger than on the HR mesh (Table 1), and in terms of degrees of freedom it fits

into the same category as $1/8^\circ$ to $1/10^\circ$ quasi-Mercator structured meshes. With the lower bound (60 km) selected on the coarser side, the Rossby-radius-based background resolution still leads to a relatively coarse mesh in the equatorial belt and subtropics, which—in retrospective—proved to be a disadvantage and has a substantial impact on the results. The main body of the analysis below serves to illustrate this point.

The FESOM-XR configuration is intended for studies with focus on high latitudes in the Northern Hemisphere, which will be reported elsewhere. Here we will largely deal only with one aspect of the simulation in this configuration that bears on the mesh design principles.

The STORM mesh follows a quasi-Mercator stretching, with bounded resolution at high latitudes of the Northern Hemisphere. It has about 5.6 M wet surface nodes, and in this sense is very similar to the FESOM-XR mesh. Note that when comparing the meshes used for FESOM and the STORM runs, we count the number of mesh vertices (which is approximately also the number of cells for STORM). One obvious difference lies in the representation of the tropics and subtropics where STORM maintains its nominal resolution whereas FESOM-XR becomes relatively coarse (Figure 1). The other obvious difference lies in the relative importance given to the two hemispheres—the strongest refinement for STORM is in the Southern Hemisphere, whereas for FESOM-XR a higher resolution is employed in the Northern Hemisphere.

3. Global SSH Variability and SST Biases

The main motivation for increasing the horizontal resolution in the open ocean is to explicitly account for mesoscale eddy dynamics. SSH variability is a good measure of the quality of the high-resolution model in simulating the surface circulation since it reflects both main pathways of major ocean currents as well as eddy activity. Figure 3 compares the variance of the sea surface height in the models to estimates obtained from satellite altimetry (AVISO, Ducet et al., 2000; Le Traon et al., 1998).

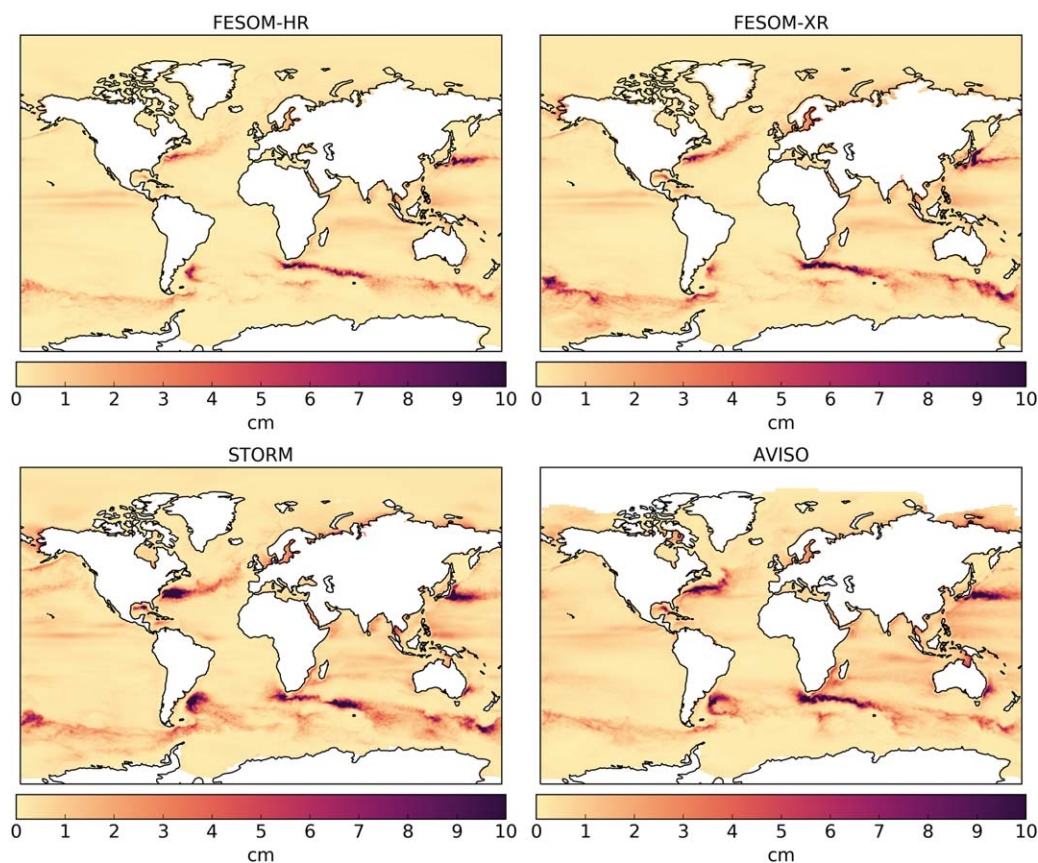


Figure 3. The sea surface height (SSH in cm) variability (i.e., the standard deviation of SSH) in models (left column) and in observations (AVISO, right column).

As is evident from Figure 3, the FESOM-HR setup underestimates SSH variability compared to AVISO. The lack of variability is especially noticeable in places where the resolution is kept relatively coarse (Figure 1, left) such as the central parts of the ocean subtropical gyres. However, even in most places where major refinements were made the simulated SSH variability remains lower than observed.

The increase in resolution in the FESOM-XR simulation leads to increased variability in energetically active ocean areas. However, small-scale variability in the centers of subtropical ocean gyres is still under-represented. Ironically, despite of the much larger node count some places (such as Brazil-Malvinas Confluence and Kuroshio) show even weaker variability compared to FESOM-HR simulation. In comparison to both FESOM simulations, STORM shows overall larger amplitudes of variability and better resolves small-scale structures visible in the AVISO data. One example is the Indian Ocean, where both FESOM simulations only show two “belts” of relatively high SSH variability, while in STORM and AVISO there is an additional “belt” between the southern tip of Madagascar and the Australian coast. On another hand, variability simulated in STORM along the Gulf Stream is too high compared to observations.

In order to see whether the variable resolution improves the quality of simulation of the sea surface temperature (SST), which is a key parameter for coupled climate simulations, we show in Figure 1 (right column) SST biases relative to the GDEM3 climatology (Carnes, 2009). The most prominent improvement in FESOM-XR compared to the FESOM-HR simulation is a considerable reduction of the negative temperature bias in the so-called “North-West corner” of the North Atlantic (will be discussed in section 4). The temperature bias in the Kuroshio extension region is reduced in FESOM-XR, but the bias around Japan becomes larger. FESOM-XR simulates a stronger positive temperature bias in the Pacific sector of the Southern Ocean. Interestingly, the STORM simulation shares its strength and structure. The appearance of this bias correlates with too high eddy variability simulated by both models in this region, and probably is related to the accompanying eddy-induced stirring.

The STORM simulation displays more warm temperature biases compared to both FESOM-HR and FESOM-XR in large part of the ocean. Note that when comparing STORM and FESOM simulation one should keep in mind the difference in the atmospheric forcing which was used to conduct the simulations (see Table 1).

To summarize, there is a small increase in the overall SSH variability in FESOM-XR compared to FESOM-HR, but it still remains lower than in the observations and in the STORM simulation on a quasi-Mercator horizontal mesh. Some local SST biases in FESOM-XR are substantially reduced, but their overall spatial structure and amplitude remains quite similar to FESOM-HR.

4. North Atlantic

The North Atlantic is a region where—based on previous studies and on our own experiences—an increase in horizontal resolution is expected to lead to significant improvements in model realism. Although some aspects of the European climate can be reproduced even in models without ocean dynamics, e.g., the winter temperature contrast between western Europe and eastern North America (Seager et al., 2002), the pattern and details of the regional SSTs impact blocking frequencies over Europe as well as the direction of storm tracks and the North Atlantic eddy-driven jet (O'Reilly et al., 2017). Despite these strong influences on the European climate, a realistic simulation of the (surface) ocean circulation in this region is still an issue of many oceanic components of global climate models. Some of the problems are related to the Gulf Stream separation, cold temperature biases in the Labrador Sea and the “zonality” of the North Atlantic current (Rackow et al., 2016; Sein et al., 2015; Sidorenko et al., 2015).

The SSH variability over the North Atlantic (Figure 4) shows that while ocean surface dynamics of the Gulf Stream and the North Atlantic current in the FESOM-XR are slightly improved compared to the FESOM-HR simulation, the SSH variability is still lower than in the observations. In particular, the variability over the Gulf Stream region after its separation is still quite small and mostly confined to the core of the current; in contrast, the variability in STORM is too strong, and is spread too much in the meridional direction. The northeastward extension of the North Atlantic current in both FESOM-HR and FESOM-XR tends to resemble the observations. XR shows stronger SSH variability than HR, which correlates with reduced errors in the Northwest Corner (see below). The North Atlantic current in the STORM simulation is way too zonal compared to the observations, especially in the central North Atlantic. In fact, STORM shows relatively strong

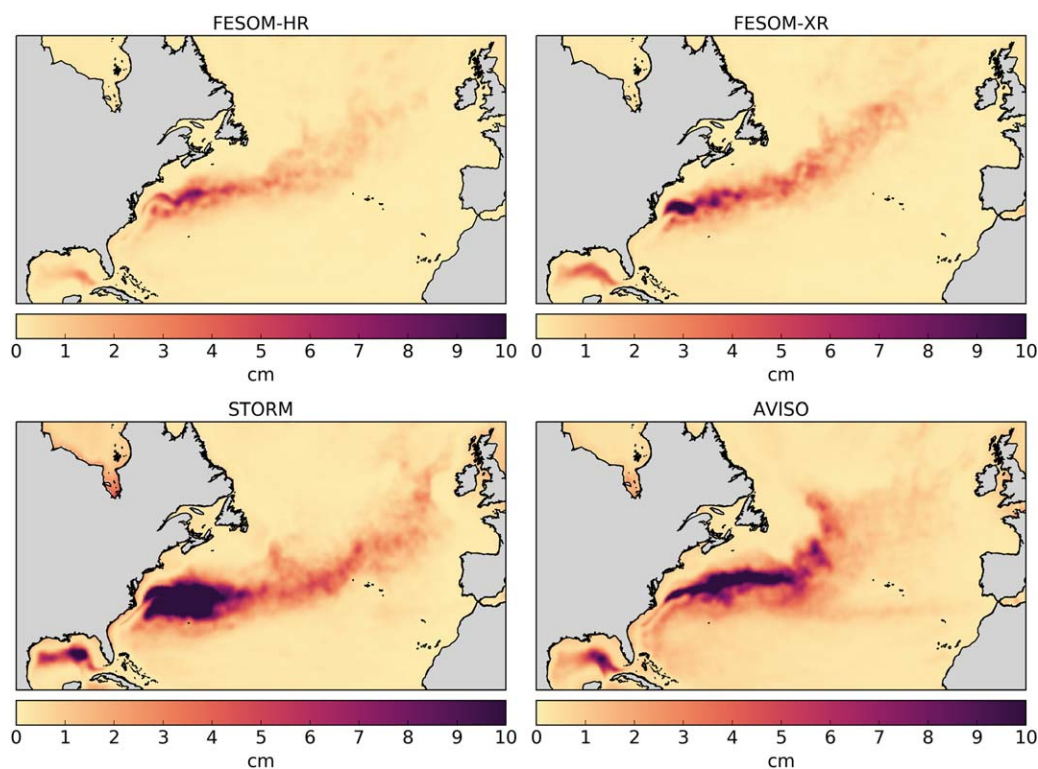


Figure 4. Same as in Figure 3, except for the North Atlantic region.

SSH variability until the British coast. All three simulations suffer from the absence of the Azores current which is clearly visible in the AVISO SSH variability.

Modeling the correct location of the Gulf Stream separation still presents a major challenge for many models (e.g., Ezer, 2016). In many simulations, the Gulf Stream continues past Cape Hatteras and only separates further north. According to the mean spatial distribution of SSH over the North Atlantic (Figure 5), the separation in both FESOM-HR and FESOM-XR happens at Cape Hatteras, as suggested by the AVISO product. However, compared to the FESOM-HR simulation, the amplitude of the meander after Cape Hatteras is smaller in XR, which presents a considerable further improvement. There is still some “looping” of the current along the coast that is absent in the observations, albeit reduced compared to FESOM-HR. This improvement mainly stems from an increase in the resolution over the shelf areas northward of the Gulf Stream front (Figure 6, left), where the cold Labrador water from the north meets the warm Gulf Stream water. An additional consequence of the increased resolution over the North American shelf is a reduction of the positive temperature bias along the US and Canadian coast (Figure 6, right).

A similar looping along the coast is also present in the STORM simulations, but the SSH gradient simulated by STORM across the Gulf Stream front is stronger and closer to the AVISO product. The STORM configuration has a uniform resolution of about 12 km over the whole North Atlantic, which is worse than in FESOM-XR over the shelf areas of the eastern North American coast, but better than in FESOM-XR further offshore. Clearly, the horizontal resolution is not the only factor influencing the simulated Gulf Stream separation. However, it leads to improvements in the considered FESOM simulations. It remains to be seen whether it is related to a reduced dissipation in the refined region, or to the improved bottom representation that is possible at higher spatial resolution.

The so-called Northwest Corner of the North Atlantic is another challenging region for ocean models. Models frequently simulate a cold surface bias in this region, which may considerably worsen the quality of simulated climate in coupled models. This problem has been frequently addressed in literature (see, e.g., Jungclaus et al., 2013; Scaife et al., 2011; Sein et al., 2015; Sidorenko et al., 2015) and originates from the wrong path of the North Atlantic current which does not properly penetrate into the Northwest Corner as it

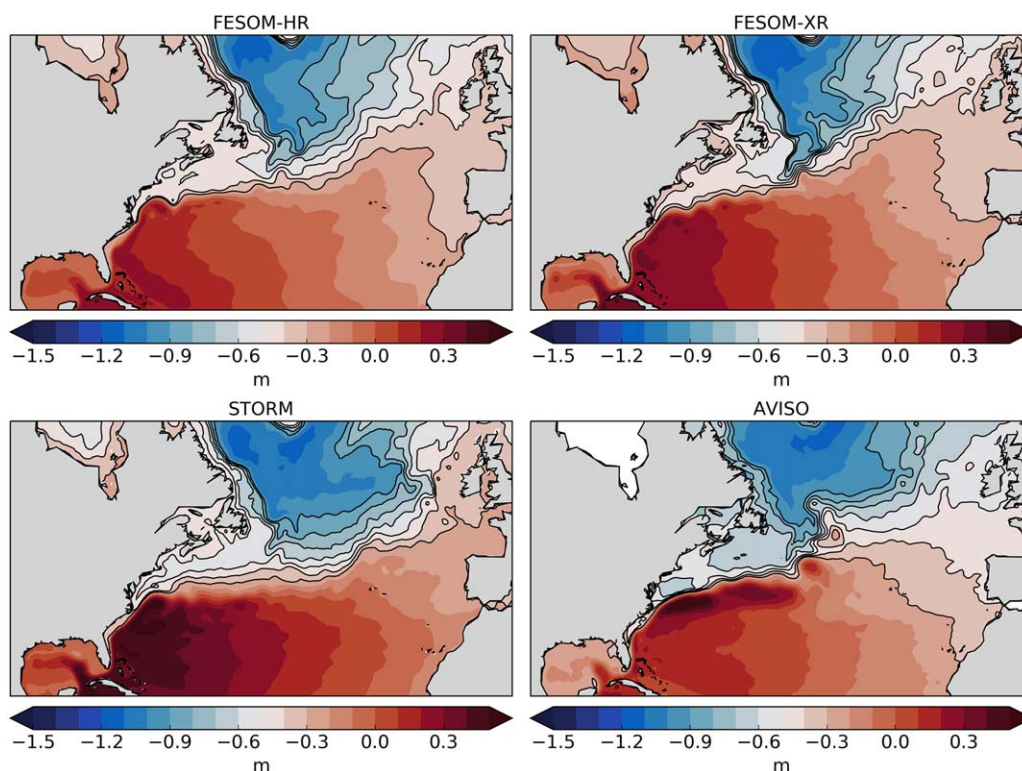


Figure 5. Mean sea surface height (in m) in the FESOM-HR/XR and STORM models and in observations (AVISO). Contour lines over color shading are drawn for levels from -0.9 to -0.3 with 0.1 interval.

is seen in observations. FESOM-XR shows notable improvement in representing this feature as compared to FESOM-HR (Figure 5). Note that the major increase in the resolution of FESOM-XR was over the shelf areas, following the “half-of-the-Rossby-radius” strategy, and that the resolution in the main flow of the North Atlantic current was only slightly increased (Figure 6, left). Interestingly, FESOM-HR and STORM share a shifted Gulf Stream front expressed in positive temperature biases off the east coast of North America. The more realistic simulation of the North Atlantic current pathway reduces the temperature bias in this region considerably (e.g., Marzocchi et al., 2015). Importantly, our notion of an improved representation of the Northwest Corner is consistent with reduced temperature biases at 100 m depth in FESOM-XR compared to FESOM-HR and STORM simulations (Figure 6, right). Accordingly, STORM does not display a good representation of the North Atlantic Current penetration toward the Northwest Corner (Figure 5).

5. Effects of Local Mesh Refinements in Dynamically Active South Atlantic Areas

Both of suggested mesh strategies lead to a creation of distinct patterns in the horizontal mesh resolution (Figure 1). In this section, we look closer at local details of the mesh refinement and their effect on the modeled circulation and surface ocean variability.

The SSH variance in the Brazil-Malvinas confluence region (Figures 2 and 7, top) in both FESOM simulations is smaller than that in STORM and AVISO data. Rather surprisingly at a first glance, FESOM-XR simulates a weaker SSH variance than FESOM-HR, although the variability at the northern flank of the Drake Passage in FESOM-XR is in good agreement with AVISO.

The horizontal resolution of FESOM-XR in the Drake Passage is comparable to that of STORM and reaches 7 km (Figure 1). However, in the Brazil-Malvinas confluence region the “half-of-the-Rossby-radius” resolution criterion used for FESOM-XR results in a relatively coarse mesh. Since it was expected that this resolution is sufficient to maintain energetic eddy dynamics, the resolution was only slightly refined using the scaling of observed SSH variability. As a result, the resolution obtained in this region remains coarse in FESOM-XR and is even coarser than in FESOM-HR. For HR, the Rossby-radius scaling was not used, and the observed

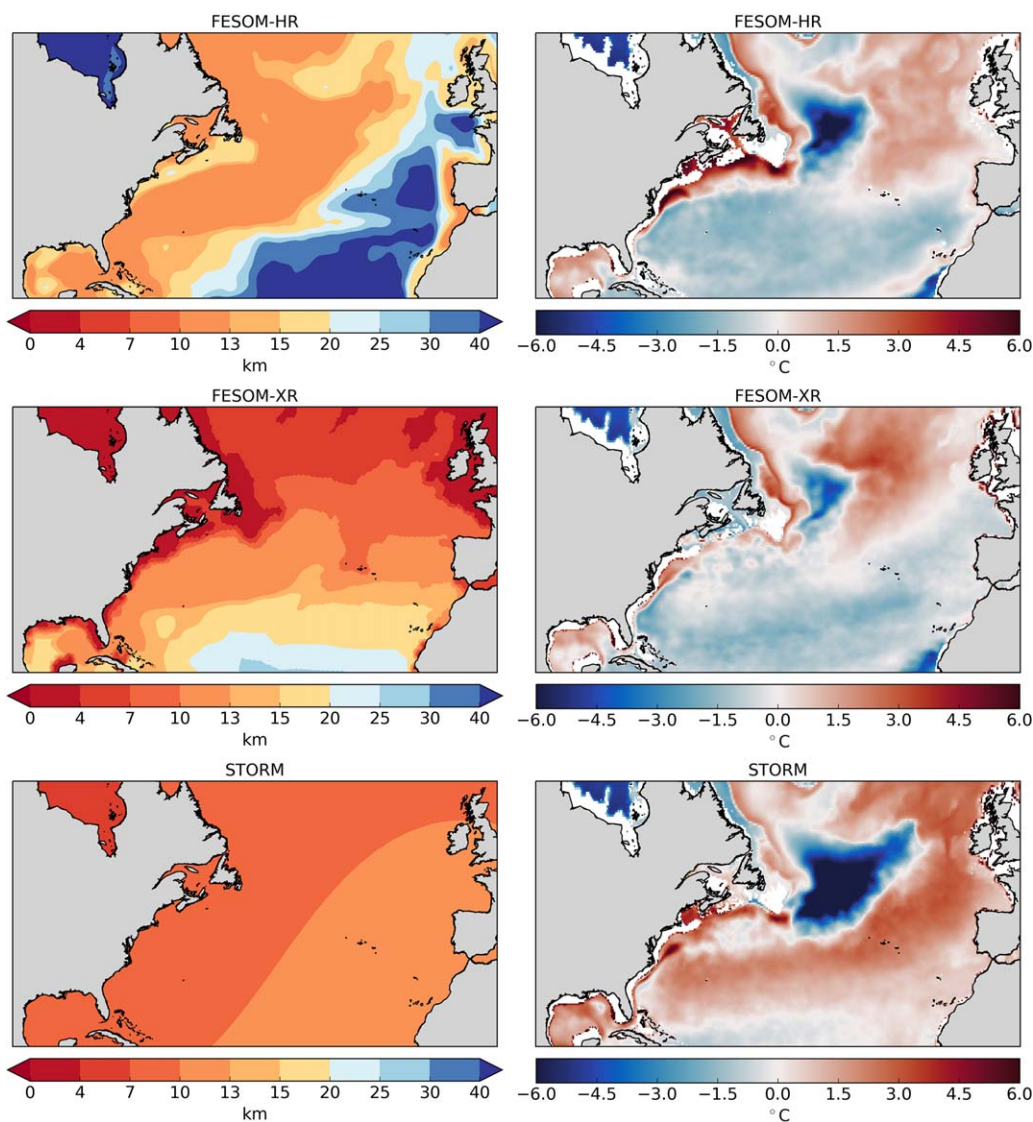


Figure 6. (left) Spatial distribution of horizontal resolution of the ocean models and (right) ocean temperature bias at 100 m with respect to the GDEM3 climatology (Carnes, 2009) in the North Atlantic region.

variability pattern was applied with a smaller threshold, resulting in higher resolution in this basin. As a consequence, the simulated SSH variability is stronger on FESOM-HR than on FESOM-XR for this particular case (Figure 3). For explicitly representing eddy dynamics, resolving the Rossby radius with two grid cells is a necessary condition for representing baroclinic instability, but not a sufficient one. We conclude that because of dissipation (viscosity and diffusion, both physical and numerical), depending on the particular location even smaller grid sizes may be needed. Furthermore, according to Soufflet et al. (2016), the scale selective dissipation is not the only factor influencing model's effective resolution, and many other factors (such as detail of time stepping) may come into play.

In the FESOM-XR mesh, the resolution stays high in the shallow part of the basin, but gets coarser, to about 15–20 km, over the Brazil-Malvinas Confluence region, which is surrounded by even coarser resolution areas toward the side of the subtropical gyre. This simply implies that resolution-related dissipation in coarse resolved surrounding destroys the variability here, despite of being appropriate in the Drake Passage area further to the south. STORM with nearly uniform horizontal resolution in this area (Figure 1, left) outperforms both FESOM setups (Figure 3).

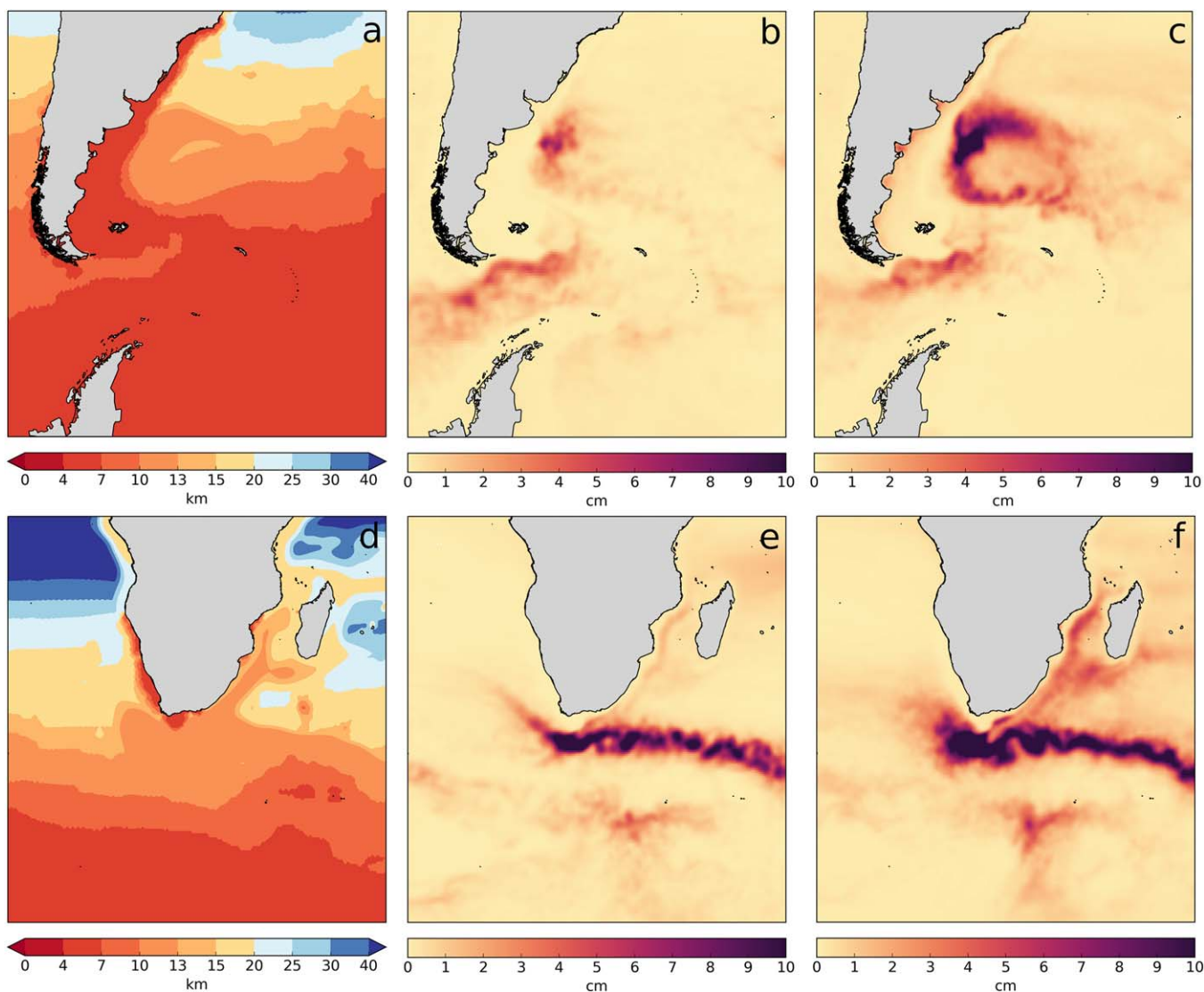


Figure 7. (a and d) Spatial distribution of horizontal resolution in FESOM-XR, (b and e) sea surface height (SSH) variability in FESOM-XR, and (c and f) AVISO. Top panels show the Brazil-Malvinas confluence region while the bottom panels display the Agulhas current region.

By following the mesh design strategy based on the observed SSH variability in combination with the Rossby-radius dependence (Figure 7a), we formally introduce relatively large irregularities into the target resolution of the FESOM-XR grid. An example for the FESOM-XR grid is the relatively highly resolved boomerang-shaped area along the slope of South America that slightly extends toward the open ocean in its northern part. Our experience with running FESOM shows, that sharp resolution jumps over regions that represent highly energetic systems turn out to be unfavorable, even when the Rossby radius is taken into account.

In our opinion, one of the main points of concern when designing a mesh is the connection between resolution and dissipation. Too sharp changes in resolution damp the effective resolution in the fine part of the mesh because eddies are dissipated stronger when they pass coarser regions. This calls for a smoother distribution of the horizontal resolution. The extent of smoothness depends on many details and in all probability varies from place to place. Further, we give one more example illustrating this behavior for the Agulhas Retroreflection region, which is another dynamically active area of the World Ocean. Here the FESOM-XR simulation shows a slight improvement in the simulated SSH variability over FESOM-HR (Figures 3 and 7, bottom), indicated by smaller difference to AVISO. The FESOM-XR configuration has a narrow band

of high horizontal resolution over the Agulhas Return Current (ARC), similar to FESOM-HR. However, compared to FESOM-HR, the resolution in the vicinity of the ARC is increased in the FESOM-XR grid, so that the simulated SSH variability along the ARC with this mesh is also increased. The resolution given by two grid cells per Rossby radius in FESOM-XR is coarser along the east coast of Africa and Madagascar than in STORM (Figure 1, left). Correspondingly, the SSH variability in this region is better simulated with STORM.

All three models have difficulties in reproducing the variability at the location of the Agulhas Retroflexion properly (Figure 3). Both FESOM configurations show an unrealistic narrow, northwesterly oriented band of SSH variability, which is a manifestation of the main travel path of the Agulhas rings. They typically turn to the north too early. Although modeling the correct path of the Agulhas rings is a common problem for many high-resolution ocean models, in FESOM-HR/XR it might be emphasized by the prescribed distribution of horizontal resolution, which stays relatively fine in the north-west direction but becomes coarser west of the retroflexion. In previous studies, it was shown that coupling with the atmosphere using climate models can improve the pathways of Agulhas eddies (McClean et al., 2011).

6. Discussions and Conclusions

6.1. Design of Local Resolution Along Main Currents

Resolution and build-in dissipation cannot be set apart because numerical codes are designed so as to dissipate the grid scale variance. A coarser mesh, even if it is Rossby-radius resolving *in the sense adopted here*, is characterized by higher dissipation, which may suppress instability or damp excessively the eddy motions originating from nearby finer regions. This is the reason why the strategy of designing meshes with grid size equal to half of the local Rossby radius, explored here with FESOM-XR, does not necessarily lead to major improvements. Our results show that SSH variability in FESOM-XR is even reduced compared to HR in places like the Brazil-Malvinas Confluence and the Kuroshio Current, because the local resolution is reduced, and resolving the Rossby radius alone is not sufficient. This result can be viewed as an illustration that the criterion of two points per Rossby radius is necessary, but not the sufficient one, and that the notion of a “Rossby-radius resolving mesh” is ambiguous on its own.

Indeed, the criterion of two grid cells per Rossby radius marks only the lower boundary; it has to be augmented by local modifications for obtaining realistic ocean setups. Besides excessive mesh coarsening toward the equator, mesh resolution simply following the scale of the Rossby radius (e.g., where shelf and deep ocean meet, and where the Rossby radius changes sharply) should be avoided. To give an example, if the resolution in the Brazil-Malvinas Confluence in the XR mesh had been designed by means of the criterion used for the HR mesh in this very region, the local SSH variability would most probably not have decreased. Different numerical codes (models) have different effective resolutions, and may require code-specific adjustments when assigning local eddy-resolving resolution (see, e.g., Soufflet et al., 2016). Recognizing all these points, we consider the results presented in this paper an important step toward understanding how to best use the potential of unstructured meshes.

6.2. Design of Resolution Surrounding Main Currents

Compared to STORM, both FESOM meshes have patches of local mesh refinement closely surrounded by coarser regions. In the Kuroshio Current region, the local resolution of two FESOM meshes is similar to that of STORM, but the SSH variability is much lower in FESOM simulations. This is because the resolution is only very locally refined along the Kuroshio Current in the North Pacific. As shown by Danilov and Wang (2015) and Sein et al. (2016), variability in the refined region can be damped if the nearby upstream region is comparably coarse. To improve future simulations of the Kuroshio Current, we need to widen the refined area and to increase resolution in the subtropical region. A topic for future studies is how FESOM simulations on a XR mesh will compare to those on an equivalent “STORM” mesh (the latter could be constructed by splitting the quadrilateral cells of STORM into triangles).

In this paper, we focus on sharing our experience about unstructured mesh design with the community, especially in the context of developing frontier meshes to be used in, for example, the HighResMIP (Haarsma et al., 2016) simulations. Since the Arctic Ocean is resolved with very high resolution in the XR simulation, one of the potential applications is to understand the Arctic Ocean dynamics and its linkage with lower latitudes.

6.3. Adapting and Static Meshes

Unstructured meshes can be made adapting to resolve the simulated dynamics using some error indicators as criteria for mesh adjustment (see, e.g., Piggot et al., 2008). In the context of mesoscale eddies it is difficult to propose an unambiguous internal error indicator function, for viscosities and diffusivities depend on resolution, and there is no convergence in a strict sense. However, the difference between the simulated and observed variability can be used to guide the design of a series of static meshes that tend to reduce the disagreement. We see this as an interesting direction, although there is the caveat that the source of errors might not necessarily be local.

Acknowledgments

The altimeter products were produced by Ssalto/Duacs and distributed by Aviso, with support from Cnes (<http://www.aviso.altimetry.fr/duacs/>). The work was supported by the EC project PRIMAVERA under the grant 641727 (D. Sein), by projects S1 (N. Koldunov) and S2 (S. Danilov) of the Collaborative Research Centre TRR 181 “Energy Transfer in Atmosphere and Ocean” funded by the German Research Foundation, by the Helmholtz Climate Initiative REKLIM (Regional Climate Change) (D. Sidorenko and Q. Wang) and by ERA-Net projects EXOSYSTEM (grant 01DJ16016) and FRAGERUS (grant 01DJ15029) funded by the Federal Ministry for Education and Research (Germany). The simulations were performed at the German Climate Computing Center (DKRZ). We thank the anonymous reviewers and the editor for the constructive suggestions and critical remarks, which helped to improve the manuscript.

References

- Carnes, M. R. (2009). *Description and evaluation of GDEM-V 3.0* (NRL/MR/7330-09-9165). Washington, DC: Naval Research Laboratory, Stennis Space Center Ms Oceanography Div.
- Danilov, S., Kivman, G., & Schröter, J. (2004). A finite-element ocean model: Principles and evaluation. *Ocean Modelling*, *6*(2), 125–150. [https://doi.org/10.1016/S1463-5003\(02\)00063-X](https://doi.org/10.1016/S1463-5003(02)00063-X)
- Danilov, S., & Wang, Q. (2015). Resolving eddies by local mesh refinement. *Ocean Modelling*, *93*, 75–83. <https://doi.org/10.1016/j.ocemod.2015.07.006>
- Ducet, N., Le Traon, P.-Y., & Reverdin, G. (2000). Global high-resolution mapping of ocean circulation from TOPEX/Poseidon and ERS-1 and 22. *Journal of Geophysical Research*, *105*, 19477–19498.
- Ezer, T. (2016). Revisiting the problem of the Gulf Stream separation: On the representation of topography in ocean models with different types of vertical grids. *Ocean Modelling*, *104*, 15–27. <https://doi.org/10.1016/j.ocemod.2016.05.008>
- Gent, P. R., & McWilliams, J. C. (1990). Isopycnal mixing in ocean circulation models. *Journal of Physical Oceanography*, *20*, 150–155.
- Griffies, S. M., Winton, M., Anderson, W. G., Benson, R., Delworth, T. L., Dufour, C. O., . . . Zhang, R. (2015). Impacts on ocean heat from transient mesoscale eddies in a hierarchy of climate models. *Journal of Climate*, *28*, 952–977. <https://doi.org/10.1175/JCLI-D-14-00353.1>
- Haarsma, R. J., Roberts, M. J., Vidale, P. L., Senior, C. A., Bellucci, A., Bao, Q., & von Storch, J.-S. (2016). High resolution model intercomparison project (HighResMIP v1.0) for CMIP6. *Geoscientific Model Development*, *9*, 4185–4208.
- Hallberg, R. (2013). Using a resolution function to regulate parameterizations of oceanic mesoscale eddy effects. *Ocean Modelling*, *72*, 92–103. <https://doi.org/10.1016/j.ocemod.2013.08.007>
- Hewitt, H. T., Roberts, M. J., Hyder, P., Graham, T., Rae, J., Belcher, S. E., . . . Wood, R. A. (2016). The impact of resolving the Rossby radius at mid-latitudes in the ocean: Results from a high-resolution version of the Met Office GC2 coupled model. *Geoscientific Model Development*, *9*, 3655–3670. <https://doi.org/10.5194/gmd-9-3655-2016>
- Jungclaus, J. H., Fischer, N., Haak, H., Lohmann, K., Marotzke, J., Matei, D., . . . von Storch, J. S. (2013). Characteristics of the ocean simulations in MPIOM, the ocean component of the MPI-Earth system model. *Journal of Advances in Modeling Earth Systems*, *5*, 422–446. <https://doi.org/10.1002/jame.20023>
- Kalnay, E., Kanamitsu, M., Kistler, R., Collins, W., Deaven, D., Gandin, L., . . . Joseph, D. (1996). The NCEP/NCAR 40-Year reanalysis project. *Bulletin of the American Meteorological Society*, *77*(3), 437–471.
- Large, W. G., & Yeager, S. G. (2009). The global climatology of an interannually varying air-sea flux data set. *Climate Dynamics*, *33*, 341–364.
- Le Traon, P.-Y., Nadal, F., & Ducet, N. (1998). An improved mapping method of multi-satellite altimeter data. *Journal of Atmospheric and Oceanic Technology*, *15*, 522–534.
- Li, H., & von Storch, J. S. (2013). On the fluctuating buoyancy fluxes simulated in a OGCM. *Journal of Physical Oceanography*, *43*(7), 1270–1287. <https://doi.org/10.1175/JPO-D-12-080.1>
- Marsland, S. J., Haak, H., Jungclaus, J. H., Latif, M., & Roeske, F. (2002). The Max-Planck-Institute global ocean/sea ice model with orthogonal curvilinear coordinates. *Ocean Modelling*, *5*(2), 91–126
- Marzocchi, A., Hirschi, J. J.-M., Holliday, N. P., Cunningham, S. A., Blaker, A. T., & Coward, A. C. (2015). The North Atlantic subpolar circulation in an eddy-resolving global ocean model. *Journal of Marine Systems*, *142*, 126–143. <https://doi.org/10.1016/j.jmarsys.2014.10.007>
- McClean, J. L., Bader, D. C., Bryan, F. O., Maltrud, M. E., Dennis, J. M., Mirin, A. A., . . . Worley, P. H. (2011). A prototype two-decade fully-coupled fine-resolution CCSM simulation. *Ocean Modelling*, *39*(1–2), 20–30.
- O’Reilly, C. H., Minobe, S., Kuwano-Yoshida, A., & Woollings, T. (2017). The Gulf Stream influence on wintertime North Atlantic jet variability. *Quarterly Journal of the Royal Meteorological Society*, *143*, 173–183. <https://doi.org/10.1002/qj.2907>
- Piggott, M. D., Pain, C. C., Gorman, G. J., Marshall, D. P., & Killworth, P. D. (2008). Unstructured adaptive meshes for ocean modeling. In M. W. Hecht & H. Hasumi (Eds.), *Ocean modeling in an eddying regime*, Geophysical Monograph 177, AGU, 383–408.
- Rackow, T., Goessling, H. F., Jung, T., Sidorenko, D., Semmler, T., Barbi, D., & Handorf, D. (2016). Towards multi-resolution global climate modeling with ECHAM6-FESOM. Part II: Climate variability. *Climate Dynamics*, *44*(3–4), 757–780 <https://doi.org/10.1007/s00382-016-3192-6>
- Ringler, T., Petersen, M., Higdon, R. L., Jacobsen, D., Jones, P. W., & Maltrud, M. (2013). A multi-resolution approach to global ocean modeling. *Ocean Modelling*, *69*, 211–232. <https://doi.org/10.1016/j.ocemod.2013.04.010>
- Roberts, M. J., Hewitt, H. T., Hyder, P., Ferreira, D., Josey, S. A., Mizielinski, M., & Shelly, A. (2016). Impact of ocean resolution on coupled air-sea fluxes and large-scale climate. *Geophysical Research Letters*, *43*, 10430–10438. <https://doi.org/10.1002/2016GL070559>
- Scaife, A. A., Copesey, D., Gordon, C., Harris, C., Hinton, T., Keeley, S., . . . Williams, K. (2011). Improved Atlantic winter blocking in a climate model. *Geophysical Research Letters*, *38*, L23703. <https://doi.org/10.1029/2011GL049573>
- Seager, R., Battisti, D. S., Yin, J., Gordon, N., Naik, N., Clement, A. C., & Cane, M. A. (2002). Is the Gulf Stream responsible for Europe’s mild winters? *Quarterly Journal of the Royal Meteorological Society*, *128*, 2563–2586. <https://doi.org/10.1256/qj.01.128>
- Sein, D. V., Danilov, S., Biastoch, A., Durgadoo, J. V., Sidorenko, D., Harig, S., & Wang, Q. (2016). Designing variable ocean model resolution based on the observed ocean variability. *Journal of Advances in Modeling Earth Systems*, *8*, 904–916.
- Sein, D. V., Mikolajewicz, U., Groeger, M., Fast, I., Cabos, W., Pinto, J. G., . . . Jacob, D. (2015). Regionally coupled atmosphere-ocean-sea ice-marine biogeochemistry model ROM. Part 1: Description and validation. *Journal of Advances in Modeling Earth Systems*, *7*, 268–304. <https://doi.org/10.1002/2014MS000357>
- Sidorenko, D., Rackow, T., Jung, T., Semmler, T., Barbi, D., Danilov, S., . . . Wang, Q. (2015). Towards multi-resolution global climate modeling with ECHAM6-FESOM. Part I: Model formulation and mean climate. *Climate Dynamics*, *44*(3), 757–780. <https://doi.org/10.1007/s00382-014-2290-6>

- Small, R. J., Bacmeister, J., Bailey, D., Baker, A., Bishop, S., Bryan, F., . . . Vertenstein, M. (2014). A new synoptic scale resolving global climate simulation using the Community Earth System Model. *Journal of Advances in Modeling Earth Systems*, *6*, 1065–1094. <https://doi.org/10.1002/2014MS000363>
- Soufflet, Y., Marchesiello, P., Lemarié, F., Jouanno, J., Capet, X., Debreau, L., & Benshila, R. (2016). On effective resolution in ocean models. *Ocean Modelling*, *98*, 36–50.
- Steele, M., Morley, R., & Ermold, W. (2001). PHC: A global ocean hydrography with a high quality Arctic Ocean. *Journal of Climate*, *14*, 2079–2087.
- von Storch, J-S., Eden, C., Fast, I., Haak, H., Hernández-Deckers, D., Maier-Reimer, E., . . . Stammer, D. (2012). An estimate of the lorenz energy cycle for the World Ocean based on the STORM/NCEP simulation. *Journal of Physical Oceanography*, *42*(12), 2185–2205. <https://doi.org/10.1175/JPO-D-12-079.1>
- Wang, Q., Danilov, S., Sidorenko, D., Timmermann, R., Wekerle, C., Wang, X., . . . Schröter, J. (2014). The Finite Element Sea Ice-Ocean Model (FESOM) v.1.4: Formulation of an ocean general circulation model. *Geoscientific Model Development*, *7*, 663–693. <https://doi.org/10.5194/gmd-7-663-2014>